ARMY RESEARCH LABORATORY

Hopkinson Bar Pulse-Shaping with Variable Impedance Projectiles—An Inverse Approach to Projectile Design

by Daniel T. Casem

ARL-TR-5246 **August 2010**

NOTICES

Disclaimers

The findings in this report are not to be construed as an official Department of the Army position unless so designated by other authorized documents.

Citation of manufacturer's or trade names does not constitute an official endorsement or approval of the use thereof.

Destroy this report when it is no longer needed. Do not return it to the originator.

Army Research Laboratory
Aberdeen Proving Ground, MD 21005-5069

ARL-TR-5246 **August 2010**

Hopkinson Bar Pulse-Shaping with Variable Impedance Projectiles—An Inverse Approach to Projectile Design

Daniel T. Casem
Weapons and Materials Research Directorate, ARL

REPORT DOCUMENTATION PAGE	Form Approved OMB No. 0704-0188

1. REPORT DATE *(DD-MM-YYYY)*	2. REPORT TYPE	3. DATES COVERED (From - To)
August 2010	Final	September 2003–January 2004

4. TITLE AND SUBTITLE
Hopkinson Bar Pulse-Shaping with Variable Impedance Projectiles–An Inverse Approach to Projectile Design

5a. CONTRACT NUMBER

5b. GRANT NUMBER

5c. PROGRAM ELEMENT NUMBER

6. AUTHOR(S)
Daniel T. Casem

5d. PROJECT NUMBER

5e. TASK NUMBER

5f. WORK UNIT NUMBER

7. PERFORMING ORGANIZATION NAME(S) AND ADDRESS(ES)
U.S. Army Research Laboratory
ATTN: RDRL-WMP-B
Aberdeen Proving Ground, MD 21005-5069

8. PERFORMING ORGANIZATION REPORT NUMBER
ARL-TR-5246

9. SPONSORING/MONITORING AGENCY NAME(S) AND ADDRESS(ES)

10. SPONSOR/MONITOR'S ACRONYM(S)

11. SPONSOR/MONITOR'S REPORT NUMBER(S)

12. DISTRIBUTION/AVAILABILITY STATEMENT
Approved for public release; distribution is unlimited.

13. SUPPLEMENTARY NOTES

14. ABSTRACT
This report discusses a pulse shaping method for the split Hopkinson pressure bar. The idea is that the profile of an incident pulse can be shaped by using an appropriately tapered projectile. A simple numerical method is described that can determine the projectile shape necessary to yield a desired pulse; it is essentially the inverse of the widely used method that determines the resulting incident pulse due to the impact of a projectile with a known shape. Examples are given where tapered projectiles are used to design tests at constant strain-rates and also to apply a sudden strain-rate "jump" to a specimen during a single test.

15. SUBJECT TERMS
Kolsky bar, split Hopkinson pressure bar

16. SECURITY CLASSIFICATION OF:			17. LIMITATION OF ABSTRACT	18. NUMBER OF PAGES	19a. NAME OF RESPONSIBLE PERSON
a. REPORT	b. ABSTRACT	c. THIS PAGE			Daniel T. Casem
Unclassified	Unclassified	Unclassified	UU	36	19b. TELEPHONE NUMBER (*Include area code*) (410) 306-0972

Standard Form 298 (Rev. 8/98)
Prescribed by ANSI Std. Z39.18

Contents

List of Figures

1. Introduction

Most Split Hopkinson Pressure Bars (SHPBs) use cylindrical projectiles to initiate a square pulse in the incident bar. This type of pulse is suitable for a wide variety of work, although it has some disadvantages. For example, the high frequency content of the signal makes it very susceptible to dispersion, with the effect that the pulse delivered to the specimen contains oscillations that are in many cases undesirable. It is also often desired to apply a constant loading rate to a specimen, or, more specifically, that a specimen be subjected to a constant strain-rate. A square pulse, in general, will not meet this requirement because of both the compliance of the bars and the lateral expansion of the sample. There is also evidence that the shape of the loading pulse can affect equilibrium conditions within a specimen, for example, see Chen et al. (*1*). It is therefore of use to have some control over the shape of the pulse, and the process of doing so is called "pulse shaping" or "wave shaping." Pulse shaping also provides flexibility to the SHPB; for example, variable strain-rates or strain-rate "jumps" can be applied (*2*).

The most common method of pulse shaping is through the use of small deformable solids placed between the projectile and the incident bar, called "pulse shapers." It is well-known that a thin copper sheet or even a few layers of paper can significantly reduce the oscillations on the incident pulse that arise due to dispersion. Slightly rounding off the impact end of the projectile achieves a similar effect. More complicated arrangements involve stacks of various pulse shapers to create different load shapes for the purpose of achieving constant strain-rates or improving conditions of specimen equilibrium (*1*, *3*, *4*).

A less used method of wave shaping is through the use of shaped projectiles; that is, projectiles whose impedances are varied in such a manner that they generate a desired waveform upon impact. An early example of this technique is Christensen and Swanson (*5*), and more recently Lok et al. (*6*). The lack of wide use of this technique is in part due to the difficulty associated with the actual fabrication of the projectiles (most likely by removing material from a piece of bar stock on a lathe). However, another problem with the method is the determination of the projectile shape needed to create a desired signal. Whereas it is fairly straightforward to predict the shape of a pulse due to impact of a projectile with known shape (by finite element analysis, for example), it is not so simple to determine the projectile shape needed to yield a specific pulse. This has been identified by Lundberg and Lesser (*7*), who term the two problems as that of *impactor analysis* and *impactor synthesis*, respectively. They note: "On physical grounds the analysis problem can generally be expected to have a solution which is unique. However, this is not the case with the synthesis problem: there may or may not exist a solution. Also, the solution, if it exists, may not be unique."

They go on to motivate the synthesis problem. "A common procedure for seeking approximate solutions of synthesis problems is to systematically solve analysis problems until (sometimes) a

satisfactory result is obtained. Of course, it is highly desirable to develop more direct methods for dealing with the synthesis problem."

In most situations with the SHPB, it is necessary to take the synthesis approach in that one has a specific pulse in mind and wants to know the projectile shape that will produce it. This report presents a numerical solution to this problem. It is based on the approximation of a tapered projectile as a series of segments of constant impedance (e.g., constant diameter), and uses one-dimensional wave propagation relations to provide a solution. A number of researchers have used this concept to model wave propagation in non-uniform bars and beams (*8–13*). In fact, Bacon (*11*) has applied this technique specifically to the problem of tapered projectiles with the SHPB, in the analysis sense, and has shown that it can yield good results. The technique discussed in this report is essentially the inverse of this method. Note that this inverse method has been used by Liu and Li (*14*) to determine projectile shapes for the SHPB, although it is currently available only in Chinese.

Section 2.1 presents the numerical solution to the analysis problem in a reasonably broad context (of which the impact problem is a special case). This is done primarily to establish the framework for the specific problem of impactor synthesis, which is presented afterwards in section 2.2. Finally, section 3 gives a number of examples that demonstrate the advantages of the method and illustrate disadvantages encountered during its application.

2. Predicting Projectile Geometry

2.1 General Analysis Problem

The general analysis problem can be stated as follows. We are given a linear elastic bar over some range $x \in [x_0, x_f]$ with variable cross-sectional area, A(x), wave speed c(x), and density, $\rho(x)$. The boundary conditions at the end of the bar are known (free surface, rigid wall, etc.). Also given are some initial distributions of axial particle velocity, v(x,0), and axial force, P(x,0). From this, it is desired to determine the velocity and force at all points at any later time t (i.e., to find v(x,t) and P(x,t) for t>0). It is assumed that the wave propagation is one-dimensional.

The idea behind the approximate solution is to divide the bar into a number of short segments over which the acoustic properties and initial conditions are approximately constant. If n is the total number of segments, each segment is denoted by S_i, where i is an integer that ranges from 1 to n. The lengths of the resulting segments are denoted Δx_i. These lengths are not, in general, constant, but are chosen such that the time needed for a wave to traverse any given segment is equal to a constant specified time interval, Δt. In other words, the lengths Δx_i are given by

$$\Delta x_i = c_i \Delta t \tag{1}$$

where c_i is the wave speed in the i^{th} segment. Similarly, the cross-sectional area and density of segment S_i are denoted as A_i and ρ_i, respectively. The impedance of S_i is therefore

$$z_i = A_i \rho_i c_i \,. \tag{2}$$

The functions for velocity and force, v(x,t) and P(x,t), are similarly discretized. Define an integer j such that

$$t = j\Delta t \,, \tag{3}$$

where j=1,2,3,...m (m is some arbitrarily large integer that corresponds to a final time), and write $v_{i,j}$ as the velocity in the i^{th} segment at time $j\Delta t$, the beginning of the j^{th} time step. Similarly, $P_{i,j}$ represents the axial force in the i^{th} segment at the beginning of the j^{th} time step. This implies that both force and velocity are constant throughout any given segment at the beginning of any time step; this is insured by the choice of segment length in equation 1. Thus, the initial conditions are now recast as

$$P_{i,0} \text{ for } i=1,2,3,...n, \text{ and}$$

$$v_{i,0} \text{ for } i=1,2,3,...n,$$

and we seek

$$P_{i,j} \text{ and } v_{i,j} \text{ for } i=1,2,...n \text{ and } j=1,2,...m.$$

The numerical solution essentially tracks the wave components due to these initial conditions as they transmit across and reflect from the interfaces between the segments. By the D'Alembert solution of the wave equation, the axial force and particle velocity in S_i at time $j\Delta t$ can be written in terms of wave components $F_{i,j}$ and $G_{i,j}$ as

$$P_{i,j} = z_i \left\lfloor F_{i,j} - G_{i,j} \right\rfloor \text{ and} \tag{4}$$

$$v_{i,j} = F_{i,j} + G_{i,j} \,. \tag{5}$$

Here $F_{i,j}$ is a wave that propagates in the direction of increasing x and $G_{i,j}$ is a wave that propagates in the direction of decreasing x. Both are square waves with units of velocity[1] and length Δx_i. Conversely, the wave components in any segment at any time can be determined from velocity and force according to

[1] It is more customary to write the components in terms of force. However, using velocity simplifies later calculations.

$$F_{i,j} = \frac{1}{2}\left[v_{i,j} + \frac{P_{i,j}}{z_i} \right], \text{ and} \tag{6}$$

$$G_{i,j} = \frac{1}{2}\left[v_{i,j} - \frac{P_{i,j}}{z_i} \right]. \tag{7}$$

Letting j=0, these equations can be used to determine the initial distributions of wave components $F_{i,0}$ and $G_{i,0}$ from the given values of $P_{i,0}$ and $v_{i,0}$. As such, $F_{i,0}$ and $G_{i,0}$ can serve as initial conditions. Similarly, if $F_{i,j}$ and $G_{i,j}$ are known for any later time step, equations 4 and 5 can be used to find $P_{i,j}$ and $v_{i,j}$. Thus the solution can be determined by tracking the progression of the wave components $F_{i,j}$ and $G_{i,j}$ as j increases from 1 to m. The key to doing this is depicted in figure 1. At any time $j\Delta t>0$, the "right moving" wave component $F_{i,j}$ in segment S_i is the sum of two waves from the preceding time step: (i) the portion of the "right moving" wave component in the segment to the left, $F_{i-1,j-1}$, that transmits across interface I_{i-1} and into S_i and (ii) the portion of the "left moving" wave in S_i, $G_{i,j-1}$, that reflects from I_{i-1} and back into S_i. This can be written as

$$F_{i,j} = F_{i-1,j-1}\vec{T}_{i-1} + G_{i,j-1}\overleftarrow{R}_{i-1} \tag{8}$$

where $\vec{T}_{i-1}$ is the coefficient of particle velocity transmission for a pulse that is incident on the I_{i-1} interface while traveling from S_{i-1} to S_i (i.e., to the "right," hence the arrow). Likewise, $\overleftarrow{R}_{i-1}$ is the coefficient of particle velocity reflection for a pulse that reflects from the I_{i-1} interface while traveling from S_i to S_{i-1} (i.e., initially propagating to the "left").

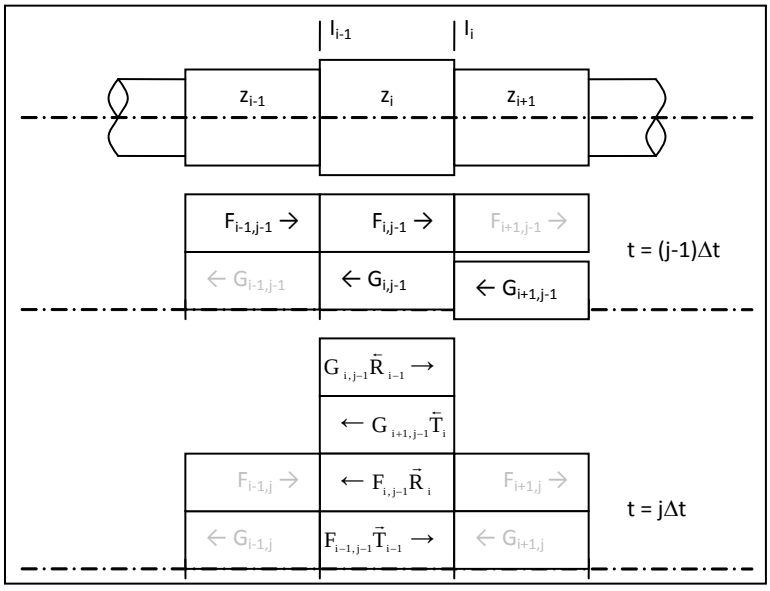

Figure 1. The F and G components at any time $j\Delta t$ are the sum of the components that transmit across or reflect from the adjacent boundaries from the previous time step. Arrows indicate direction of propagation.

In a similar manner, the left moving wave component in S_i at time $j\Delta t$, denoted by $G_{i,j}$, can be written as the sum of the components of the two waves in the previous time step that (i) transmit from S_{i+1} across interface I_i and into S_i and (ii) reflect from I_i while traveling from S_i to S_{i+1} (but of course reverses direction upon reflection).

$$G_{i,j} = G_{i+1,j-1}\overleftarrow{T}_i + F_{i,j-1}\vec{R}_i \ . \tag{9}$$

The coefficients $\overleftarrow{T}_i$ and $\vec{R}_i$ are defined similarly as above. Thus for any given interface, there are four coefficients of interest, $\vec{T}_i$, $\vec{R}_i$, $\overleftarrow{T}_i$, and $\overleftarrow{R}_i$. Assuming that the segments remain in contact at all times, the coefficients for any interface I_i can be related to the impedances of the adjacent segments as follows, for example, refer to Gaff (*15*).

$$\vec{T}_i = \frac{2z_i}{z_i + z_{i+1}} \tag{10}$$

$$\vec{R}_i = \frac{z_{i+1} - z_i}{z_i + z_{i+1}} \tag{11}$$

$$\overleftarrow{T}_i = \frac{2z_{i+1}}{z_i + z_{i+1}} \tag{12}$$

$$\overleftarrow{R}_i = \frac{z_i - z_{i+1}}{z_i + z_{i+1}} \tag{13}$$

Since z_i is given for all i, these are known quantities. It is also useful to note the following relations between the interface coefficients.

$$\vec{R}_i = \vec{T}_i - 1, \tag{14}$$

$$\overleftarrow{T}_i = 2 - \vec{T}_i, \tag{15}$$

and

$$\overleftarrow{R}_i = 1 - \vec{T}_i. \tag{16}$$

The solution now proceeds as follows. Using the initial conditions $P_{i,0}$ and $v_{i,0}$, the initial distributions of $F_{i,0}$ and $G_{i,0}$ are determined from equations 6 and 7. Then, for the first time step (j=1), the values of $F_{i,1}$ and $G_{i,1}$ are found from $F_{i,0}$ and $G_{i,0}$ for all i by equations 8 and 9.[2] The same equations are then used to determine $F_{i,2}$ and $G_{i,2}$ in terms of $F_{i,1}$ and $G_{i,1}$. This is continued for j=3,4,...m. At any time, equations 4 and 5 can be used to determine force and velocity, and thus the desired solution is obtained. Note that it is possible to simplify this solution considerably by eliminating $F_{i,j}$, $G_{i,j}$, $\vec{T}_i$, $\vec{R}_i$, $\overleftarrow{T}_i$, and $\overleftarrow{R}_i$ in favor of $P_{i,j}$, $v_{i,j}$, and z_i (*10*, *11*).

[2]Specialized equations for the boundaries of the system (I_0 or I_n) do not need to be considered here.

However, for clarity in the next section, it is easier to leave them in the present form. It should also be noted that for any given time step, the solution over the entire bar is obtained from the previous time step, and requires only n implementations of equations 8 and 9, one for each segment. Thus, the solution proceeds very quickly, and it is not unreasonable to discretize the system into thousands of segments when the technique is performed on a computer.

2.2 Projectile Impact

In this section, attention is focused on the special case of a projectile of variable impedance striking a semi-infinite bar of constant impedance. In the analysis case, the impedance variation of the striker is given and we seek the force and velocity it exerts on the bar, (i.e., $P_{0,j}$ and $v_{0,j}$). In the synthesis case, we are given the desired impact force, $P_{0,j}$, and seek the variation of impedance to produce it. The analysis version can be easily obtained by tailoring the general analysis case, previously discussed, with the specific conditions of the impact problem. In other words, one simply assigns impedances and initial conditions to the segments and proceeds with the solution. However, the same is not true for the synthesis problem. Although it is possible to pose the approximate solution to a "general synthesis" problem, it is fairly difficult to then reduce it to the special case of projectile impact. An easier approach is to develop the equations for the impact analysis problem from a slightly different perspective than that above, and then determine the inverse from it. For this reason, both methods are developed in parallel in this section.

Consider the projectile-bar system segmented as shown in figure 2. The projectile consists of n segments labeled S_{-n}, S_{-n+1}, ... S_{-1}. The use of negative subscripts for i, although slightly awkward, is done so that the target bar always begins at S_0 and the projectile initially travels to the right. The semi-infinite bar is represented by all segments for which $i \geq 0$, and the void behind the projectile is represented by all segments for which $i < -n$. The initial velocity of the projectile, v_p, must be given in either the analysis or synthesis case. Similarly, the impedance of the bar, z_{bar}, must be given in either case.

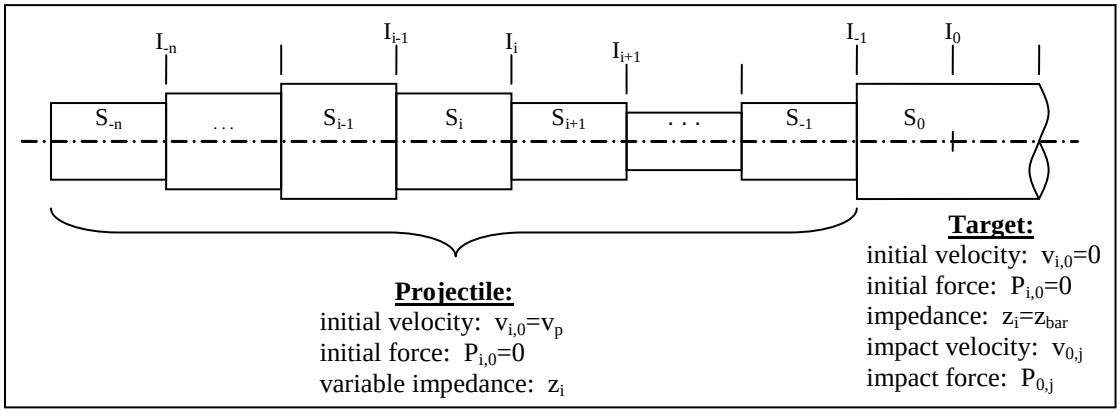

Figure 2. A segmented projectile strikes a semi-infinite bar of known impedance at a velocity v_p.

Additional quantities of interest are the impedances of the projectile, z_{-n}, z_{-n+1}, ...z_{-1}, and the particle velocity of the first segment of the bar for all time, $v_{0,j}$.[3] To summarize, we have the following:

impedances:

$$z_i = \begin{cases} 0 & \text{for } i<-n \\ \text{unknown or given} & \text{for } i \in [-n,-1], \\ 1 & \text{for } i\geq 0 \end{cases} \tag{17}$$

initial velocity:

$$v_{i,0} = \begin{cases} 0 & \text{for } i<-n \\ v_p & \text{for } i \in [-n,-1], \\ 0 & \text{for } i\geq 0 \end{cases} \tag{18}$$

initial axial force:

$$P_{i,0} = 0 \text{ for all } i, \tag{19}$$

velocity of segment 0:

$$v_{0,j} = \text{given or unknown for } j>0. \tag{20}$$

It is easier to deal with the interface parameter $\vec{T}_i$ instead of z_i. By equations 10 and 17, we write the following:

$$\vec{T}_i = \begin{cases} 1 & \text{for } i<-n-1 \text{ (100\% transmission between void segments)} \\ 0 & \text{for } i=-n-1 \text{ (the non-impacting end of the projectile)} \\ \text{unknown or given} & \text{for } i \in [-n,-1] \\ 1 & \text{for } i\geq 0 \text{ (100\% transmission between bar segments).} \end{cases} \tag{21}$$

These are of course known by equation 10 in the analysis problem, and can serve as unknowns in the synthesis problem (from which equation 10 can be used to find the impedance values). Recall the remaining interface coefficients are related to $\vec{T}_i$ by equations 14 through 16.

It is also easier to redefine the initial conditions of equations 18 and 19 in terms of $F_{i,0}$ and $G_{i,0}$. By equations 6 and 7, the new initial conditions are obtained.

[3] It is sufficient to deal with $v_{0,j}$. Although $P_{0,j}$ may be preferred, it can always be related to $v_{0,j}$ by $P_{0,j}=z_0 v_{0,j}$ since z_0 is known.

$$F_{i,0} = G_{i,0} = \begin{cases} \frac{1}{2} v_p & \text{for } i \in [-n,-1] \\ 0 & \text{for all other i .} \end{cases} \tag{22}$$

At this point it is necessary to relate the velocity profile, $v_{0,j}$, to the transmission coefficients $\vec{T}_i$. This is done by rewriting equation 5 for S_0 for all j>0. That is, for j=1,2,...m,

$$v_{0,j} = F_{0,j} + G_{0,j} = F_{0,j} . \tag{23}$$

Here the observation has been made that $G_{0,j}$ is zero for all time because it represents a left-moving wave in S_0. A non-zero $G_{0,j}$ implies that waves transmitting into the target bar somehow reflect and return to its impact end, an impossibility. Although the development that follows shows this, imposing this condition now greatly simplifies later calculations.

Equation 23 can be used to generate the desired relations provided the definitions used in equations 8 and 22 are used to expand $F_{0,j}$ in the following way:

$$F_{i,j} = \begin{cases} F_{i-1,j-1}\vec{T}_{i-1} + G_{i,j-1}\overleftarrow{R}_{i-1} & \text{for } j>0, \text{ all i} \\ v_p/2 & \text{for } j=0 \text{ and } i \in [-n,-1] \\ 0 & \text{for } j=0 \text{ and } \{i<-n \text{ or } i\geq 0\} . \end{cases} \tag{24}$$

What this means is that for some non-zero value of j, equation 23 is expanded "backwards" in time by successive substitutions of equation 24 until it is written in terms of v_p, the initial known projectile velocity (note how $F_{i,j}$ is written in terms of wave components from the previous time step). This also requires a similar expansion of $G_{i,j}$ which can be defined by equations 9 and 22.

$$G_{i,j} = \begin{cases} G_{i+1,j-1}\overleftarrow{T}_i + F_{i,j-1}\vec{R}_i & \text{for } j>0, \text{ all i} \\ v_p/2 & \text{for } j=0 \text{ and } i \in [-1,-n] \\ 0 & \text{for } j=0 \text{ and } \{i<-n \text{ or } i\geq 0\} . \end{cases} \tag{25}$$

To illustrate the application of this procedure, we now assume a projectile of at least two segments ($n\geq 2$) and develop equation 23 for j=1, 2, 3, and 4. For j=1, we have

$$v_{0,1} = F_{0,1} . \tag{26}$$

By equation 24, this becomes

$$v_{0,1} = F_{-1,0}\vec{T}_{-1} + G_{0,0}\overleftarrow{R}_{-1} . \tag{27}$$

By use of equations 24 and 25, $F_{-1,0}$ and $G_{0,0}$ can be written in terms of v_p to yield

$$v_{0,1} = \frac{1}{2} v_p \vec{T}_{-1} \ . \tag{28}$$

Therefore if $v_{0,1}$ is known we can find $\vec{T}_{-1}$ and vice versa. In other words, the first time step is used to relate the velocity in S_0 to the interface coefficient immediately to the left of the bar. In the synthesis case, since z_0 is known, this can be used to solve for z_{-1}. Note that $v_{0,1}$ and $\vec{T}_{-1}$ are linearly related.

Next, for j=2, equation 23 is expanded in three steps. The first use of equation 24 yields

$$v_{0,2} = F_{0,2} = \left[F_{-1,1} \vec{T}_{-1} + G_{0,1} \overleftarrow{R}_{-1} \right] . \tag{29}$$

Next $F_{-1,1}$ and $G_{0,1}$ are expanded using equations 24 and 25, respectively.

$$v_{0,2} = \left[F_{-2,0} \vec{T}_{-2} + G_{-1,0} \overleftarrow{R}_{-2} \right] \vec{T}_{-1} + \left[G_{1,0} \overleftarrow{T}_0 + F_{0,0} \vec{R}_0 \right] \overleftarrow{R}_{-1} \ . \tag{30}$$

Now all wave components are in terms of j=0, so the final expressions in equations 24 and 25 apply.

$$v_{0,2} = \left[\frac{1}{2} v_p \vec{T}_{-2} + \frac{1}{2} v_p \overleftarrow{R}_{-2} \right] \vec{T}_{-1} + \left[0 + 0 \right] \overleftarrow{R}_{-1} = \frac{1}{2} v_p \left[\vec{T}_{-2} + \overleftarrow{R}_{-2} \right] \vec{T}_{-1} \ . \tag{31}$$

On the surface, it appears that this equation relates $v_{0,2}$ and $\vec{T}_{-2}$ (since $\vec{T}_{-1}$ is known and $\vec{T}_{-2}$ and $\overleftarrow{R}_{-2}$ are not independent), and can be used to solve for the former or the latter in the analysis and synthesis cases, respectively. However, by equation 14, the quantity in the brackets on the right hand side is unity and we are left with

$$v_{0,2} = \frac{1}{2} v_p \vec{T}_{-1} \text{ or} \tag{32}$$

$$v_{0,2} = v_{0,1} \ . \tag{33}$$

This result has no major consequence in the analysis case, as the expansion of $v_{0,2}$ will always yield this result. However, in the synthesis case, this equation provides no useful information, i.e., it cannot be used to solve for any $\vec{T}_i$. Furthermore, it places a restriction on the velocity profile $v_{0,1}$, $v_{0,2}$,...$v_{0,j}$ that may be prescribed, namely that $v_{0,2} = v_{0,1}$.

We next perform the expansion of equation 23 for j=3 and obtain, after considerable simplification,

$$v_{0,3} = \frac{1}{2} v_p \left[\left[\vec{T}_{-3} + \overleftarrow{R}_{-3} \right] \vec{T}_{-2} + \vec{R}_{-1} \overleftarrow{R}_{-2} \right] \vec{T}_{-1} + \frac{1}{2} v_p \vec{T}_{-1} \vec{R}_0 \overleftarrow{R}_{-1} \ . \tag{34}$$

As above, this expression is deceptive because at first glance it seems that $v_{0,3}$ is related to interface coefficients for I_{-3}, I_{-2}, I_{-1}, and I_0. This is fine in the analysis case but would involve

two unknowns in the synthesis case (i.e., $\vec{T}_{-3}$ and $\vec{T}_{-2}$ are both yet to be determined). Fortunately, equation 14 again applies and equation 34 reduces to

$$v_{0,3} = \frac{1}{2} v_p \left[2\vec{T}_{-2} + \vec{T}_{-1} - \vec{T}_{-1}\vec{T}_{-2} - 1 \right] \vec{T}_{-1} \ , \tag{35}$$

where equations 11 and 13 have been used for further simplification. The end result for the synthesis problem is that equation 23 for j=3 can be used to find $\vec{T}_{-2}$, the interface coefficient for the interface one segment to the left of impact surface. Since z_{-1} is known from the first time step, equation 10 can be used to find z_{-2}. Also note that just as $v_{0,1}$ is linearly related to $\vec{T}_{-1}$, $v_{0,3}$ is linearly related to $\vec{T}_{-2}$.

This process can be continued for j=4. After exhausting applications of equations 24 and 25 and simplification with equations 14–16, we have

$$v_{0,4} = \frac{1}{2} v_p \left[2\vec{T}_{-2} + \vec{T}_{-1} - \vec{T}_{-1}\vec{T}_{-2} - 1 \right] \vec{T}_{-1} \ . \tag{36}$$

Comparison with equation 35 shows that

$$v_{0,4} = v_{0,3} \tag{37}$$

in analogy with equation 33. Thus neither the j=2 or the j=4 time steps can be used to solve for any interface coefficient.

At this point, two trends of the solution to the synthesis problem begin to emerge. The first is that the velocity profile exerted on the bar is subject to the condition that

$$v_{0,j} = v_{0,j+1} \ \text{ for } \ j = 1,3,5,.... \ . \tag{38}$$

The second stems from the observation that the expansion of $v_{0,1}$ is used to solve for $\vec{T}_{-1}$ and z_{-1}, and the expansion of $v_{0,3}$ is used to solve for $\vec{T}_{-2}$ and z_{-2}. In general, $v_{0,j}$ can be used to solve for $\vec{T}_{-(j+1)/2}$ for all odd values of j. In this manner, $v_{0,5}$ is used to solve for $\vec{T}_{-3}$, $v_{0,7}$ is used to solve for $\vec{T}_{-4}$, etc, i.e., every other time step is used to determine the next interface coefficient away from the impact interface (as well as the impedance value that is associated with it).

Both of these trends can be explained by detailed expansion of equation 23 for j=5, 6, 7, etc., a time-consuming endeavor. It is therefore preferable to justify them based on the physics of the problem. Without question, the terms in these expansions represent the propagation of various wave components throughout the system. To see this, equation 23 is re-expanded for j=3, but without the final substitution of ½v_p for $F_{i,0}$ and $G_{i,0}$. The result is

$$v_{0,3} = F_{-3,0}\vec{T}_{-3}\vec{T}_{-2}\vec{T}_{-1} + G_{-2,0}\vec{R}_{-3}\vec{T}_{-2}\vec{T}_{-1} + F_{-1,0}\vec{R}_{-1}\vec{R}_{-2}\vec{T}_{-1} \ . \tag{39}$$

Each of the three terms on the right hand side represents the portion of a wave that propagates across three segments of the projectile to reach the bar at the beginning of the third time step. So the first term, for example, represents the portion of the original right-moving wave in S_{-3} that transmits through I_{-3}, through I_{-2}, through I_{-1}, and finally into S_0 to contribute to the impact velocity $v_{0,3}$. Similarly, the second term is the portion of the left-moving wave initially in S_{-2} that reflects from I_{-3} back into S_{-2}. It then transmits across I_{-2} and I_{-1} and into the bar. Referring to figure 2, it is not difficult to see that these three terms represent all possible paths that a wave initiating in the projectile can reach the bar interface in exactly three time steps.[4] It is therefore reasonable to expect a certain amount of causality between a distant interface and the time at which it has influence on the velocity profile at the impact interface. This manifests itself in the observation that later time steps are used to solve for more distant interface coefficients. Since the segment lengths are chosen so that any given wave travels one segment per time step, it might be anticipated that each successive time step should provide the solution for one interface coefficient, each exactly one segment further away from the previous (j=1 determines $\vec{T}_{-1}$, j=2 determines $\vec{T}_{-2}$, etc.). In a more general case this is true.[5] However, this is not the case for the impact problem, where it is apparent that only the odd time steps are used to obtain the unknown coefficients.

The reason for this has to do with the initial conditions of the projectile. Consider for a moment a non-uniform projectile that does not strike a bar. Without an impact, it remains at a constant uniform velocity for all time, as well as remaining free from axial force. Since from our frame of reference the projectile has a velocity v_p, the only way for this to occur is if $F_{i,j} = G_{i,j} = \frac{1}{2}v_p$ for all time. This can be verified directly from equations 4 and 5. This means that the propagation of wave components from segment to segment, as governed by equations 8 and 9, must be such that the values of the components remain equal to $\frac{1}{2}v_p$. That this is the case can be seen directly from equations 8 and 9 after eliminating the interface coefficients (by equations 14–16) in favor of the preferred coefficients $\vec{T}_i$ and $\vec{T}_{i-1}$. These equations are, respectively,

$$F_{i,j} = \vec{T}_{i-1}\left[F_{i-1,j-1} - G_{i,j-1}\right] + G_{i,j-1} \text{ and} \tag{40}$$

$$G_{i,j} = \vec{T}_i\left[F_{i,j-1} - G_{i+1,j-1}\right] + 2G_{i+1,j-1} - F_{i,j-1}. \tag{41}$$

Clearly, if all components at time j-1 are equal to $\frac{1}{2}v_p$, these equations lead to the result that the components at time j are also equal to $\frac{1}{2}v_p$. This is true regardless of the values of the interface coefficients (i.e., *the propagation of the velocity components proceeds independently of the*

[4] It is possible to develop this solution technique based on this idea.

[5] A more general problem might have the impedances of segments on both sides of S_0 unknown, arbitrary initial distributions of force and velocity given, and the force and velocity at S_0 specified for all time. In this problem it can be shown that the expansion of $F_{0,j}$ determines z_{-j} (the impedance values for all segments to the left of S_0) and the expansion of $G_{0,j}$ determines z_j (the impedance values of all segments to the right). This assumes the given information meets certain conditions.

projectile shape.) This is a reasonable result, as it is not expected that a non-uniform velocity would spontaneously develop within a projectile that travels by simple rigid body translation and free from external influence.

The effect on the synthesis problem is as follows. A given wave component propagates independently of the local interface coefficients up until the time the propagation begins to deviate from "uniform motion." The only way for this to happen is through the action of the target, which transmits a wave into the projectile at a speed of one segment per time step. Once this wave reaches a segment, the propagation is then dependent on the local interface coefficients. However, this dependence will not influence the loading of the target until this wave travels back to the impact surface.

Consider, for example, the I_{-3} interface. During the time leading up to the 3rd time step, a wave propagates from S_{-3} to the projectile-bar interface and contributes to $v_{0,3}$. In doing so, it crosses I_{-3}. But because this crossing occurs during the first time step, the effect of the impact has yet to reach S_{-3} (because the wave front is still one segment away). Because of this, S_{-3} is still behaving as a simple projectile, and the local propagation occurs independently of the value of the I_{-3} coefficients. It is not until j=5, when part of the impact wave has had time to travel from S_0 to I_{-3}, reflect, and travel back to S_0, that the impact velocity profile depends on the nature of the I_{-3} interface. The result is that the j=5 time step is used to determine the $\vec{T}_{-3}$.

This same reasoning helps explain why the even values of j do not lead to useful equations. Consider the propagation of the impact wave into the projectile for j=4. $\vec{T}_{-2}$ has been determined during the previous time step, and so the next unknown is $\vec{T}_{-3}$. During the first four time steps, the wave front has only enough time to cross S_{-1} and S_{-2}, reflect from I_{-}, and travel back to S_{-1}. Another time step is needed for the link to S_0 to occur, and so no information about $\vec{T}_{-3}$ is gained. Instead, we obtain the result that $\vec{T}_{-3} = \vec{T}_{-4}$. It is not hard to see that this argument holds for any other even value of j.

A final important note is that, in the synthesis problem, a projectile of n segments is completely determined by the specification of $v_{0,j}$ over m time steps provided

$$m = 2n . \tag{42}$$

This is in accordance with the fact that only every other time step determines an unknown (i.e., the number of available equations matches the number of unknowns). Furthermore, if one were to specify velocity conditions beyond this time the problem would not be well-posed and could not be fully solved. Therefore, m must be selected to satisfy equation 42. It is somehow not surprising that this time corresponds to the time needed for a wave to travel down the projectile and back. However, this is not to say that the signal delivered to the bar is zero for times greater than $m\Delta t$ because in general it is not. This has important implications to the SHPB and is discussed in section 3.

Finally, it is noted that during the solution process, $v_{0,j}$ is always linearly related to $\vec{T}_{-(j+1)/2}$ (j odd). This can be seen directly from the linearity in equations 24 and 25. It is true that during substitution into equation 23 these equations become "nested" in such a way that higher order relationships between the impact velocity and interface coefficients emerge, but this only occurs at times beyond which the coefficient is determined.[6] Since an unknown coefficient $\vec{T}_i$ is determined by the expansion equation in which $\vec{T}_i$ makes its first non-canceling appearance, the relationship between $\vec{T}_i$ and the corresponding given value of $v_{0,j}$ is always linear. The reason this fact is mentioned is that it is exploited in the numerical solution discussed below.

Programming Aspects

Although the application of this procedure may appear cumbersome, it is very easy to program. An example is given in the appendix. All that needs to be done is to define the initial conditions, define functions for equations 24, 25, and 14–16, and then solve equation 23 as j = 1, 3, 5,...2n for the unknown transmission coefficients. The fact that, for any odd time step, $\vec{T}_{-(j+1)/2}$ is linearly proportional to $v_{0,j}$ can be used to simplify the programming. Although it may be possible to solve the expanded equations directly for $\vec{T}_{-(j+1)/2}$, it does not appear trivial and in any case was not seriously investigated during this research. Instead, equation 23 is solved twice for each odd time step using two different assumed values of $\vec{T}_{-(j+1)/2}$, for example, $\vec{T}'_{-(j+1)/2} = 0$ and $\vec{T}''_{-(j+1)/2} = 2$. This gives two values for the velocity profile, $v'_{0,j}$ and $v''_{0,j}$. The actual value of $\vec{T}_{-(j+1)/2}$ is found by linear interpolation,

$$\vec{T}_i = \vec{T}'_i + \left(\vec{T}''_i - \vec{T}'_i\right)\frac{v_j - v'_j}{v''_j - v'_j} \quad , \tag{43}$$

where j is odd and i=-(j+1)/2. The only drawback is that two calculations of equation 23 are required per time step.

It is clear from the nature of the substitutions that the number of terms in the expansion of $v_{0,j}$ doubles with each increase in j. This results in a growth of a factor of four between the odd time steps. So although there is only one term in the expression for $\vec{T}_{-1}$, there are four for the expression for $\vec{T}_{-2}$, 16 for the expression for $\vec{T}_{-3}$, etc. The solution rapidly becomes cumbersome. However, continual expansion back to component values at j=0 involves a large number of re-solving of terms. By simply keeping track of which $F_{i,j}$ and $G_{i,j}$ have been solved during the solution process, a great computational savings is gained and the solution of the

[6]For example, $\vec{T}_1$ is linearly related to $v_{0,1}$ in equation 28, but non-linearly related to $v_{0,2}$ in equation 35. However, since equation (35) is an expression for j=3, $\vec{T}_1$ should have already been determined.

synthesis problem is not much more expensive than that of the analysis problem.[7] This is an advantage over techniques which use iterations of the analysis problem to solve the synthesis problem.

3. Applications

Two practical applications of shaped projectiles are given in this section, both applied to the SHPB. First, however, several important caveats of the method are discussed.

3.1 Determination of Projectile Area

The synthesis method of section 2.2 only determines the projectile impedance; more information is required to determine the density, wave speed, and area. This additional complication is avoided if one chooses beforehand to use a specific uniform projectile material (e.g., the same material as the bar). But the ability to use other materials or even multiple materials adds flexibility to the method.

3.2 Constraint of Gun Barrel Diameter

SHPB projectiles are most commonly fired from gas guns. This means that the outer diameter of the projectile must fit the barrel of the gun, either on its own accord or through the use of sabots. This imposes an additional constraint on the synthesis problem. In other words, when a projectile shape is determined to yield a specific incident pulse, there is no guarantee that it will fit the gun. Fortunately, in most cases it is possible to adjust the assumed impact velocity v_p to either increase or decrease the maximum projectile diameter accordingly. This involves re-solving the synthesis problem, and usually requires a few iterations of v_p to determine a projectile with an outer diameter that matches the gun. Of course, since the projectile must match the gun at a minimum of two points along its length, a sabot may still be required. It is worth mentioning that it is possible to reduce the projectile area by boring a hole at one end (at least partially) instead of removing material from the outside. This way, the area can be reduced while preserving the outer diameter, and it may be possible to avoid the use of sabots entirely.

3.3 Incomplete Momentum Transfer

Most readers are probably familiar with the standard SHPB projectile which has the same cross-sectional area as the bar and is made from the same material. This projectile, upon impact, transfers all of its momentum to the incident bar and comes to a complete stop. The duration of the pulse delivered to the bar is exactly twice the length of the projectile. Unfortunately, this is not the case with a tapered projectile. As mentioned at the end of section 2.2, the interaction between the projectile and bar does not end after two transits along the projectile ($t=2n\Delta t$). This

[7] For simplicity, the program in the appendix does not include such a scheme, and is therefore cumbersome to run even for modest values of n.

means one of two things: the projectile either continues to move forward or it bounces back. The first case could be problematic if the incident pulse cannot be separated from its reflection in the subsequent analysis. For this reason, the second case, where the projectile rebounds, is ideal.[8] However, depending on the exact conditions of the impact, the speed of the rebounding projectile may be considerable and possibly damaging to the gas gun that fired it. It is therefore recommended that after a projectile shape has been determined, the corresponding analysis problem be solved to determine the action of the projectile beyond the $2n\Delta t$ time period. In this regard, a finite element simulation might be preferred over the analysis method of section 2.1 because it can allow the projectile and bar to separate (the method of section 2.1 will instead transmit a tensile pulse to the bar).[9]

4. Pulse Shaping for Constant Strain-Rate

Part of the impetus for this research developed during a program that involved the measurement of adiabatic stress-strain curves at constant rates of true strain in the SHPB. This can be achieved by tailoring an incident pulse to suit the deformation of a particular specimen. Once a specimen in a SHPB attains equilibrium, the engineering stress within the sample is uniform and equal to the stress on the incident bar, scaled by the ratio of the bar area to that of the specimen, for example, refer to Meyers (*16*).[10]

$$s_S = \frac{A_B}{A_S}\left[\sigma_I + \sigma_R\right]. \tag{44}$$

Here σ_I and σ_R are the bar stresses due to the incident and reflected pulses at the time they act at the specimen interface. s_S is the specimen engineering stress, and A_S and A_B are the initial cross-sectional areas of the specimen and bar, respectively.

Similarly, the engineering strain-rate within the specimen can be found from the reflected pulse.

$$\dot{e}_S = \frac{-2}{L_S \rho c_0}\sigma_R . \tag{45}$$

Here L_S is the initial length of the specimen, and ρ and c_0 are the density and bar wave speed of the bar.

If the specimen stress is known, these equations can be solved to give the incident pulse needed to yield a test at a desired strain-rate.

[8] If one starts with a projectile that is the same material and diameter as the bar and only removes material the resulting tapered projectile will rebound after one transit.

[9] A finite element analysis is also a reliable way to make sure that the bar and projectile remain elastic (e.g., a projectile with a very narrow tip could unexpectedly yield upon impact).

[10] Note all stress and strain quantities are assumed positive in compression.

$$\sigma_I = \frac{A_S}{A_B} s_S + \frac{L_S \rho c_0}{2} \dot{e}_S \ . \tag{46}$$

This gives the profile needed to produce a test at the given engineering strain-rate $\dot{e}_S$, which can be chosen constant.

In many cases, it is preferable to work with data at constant rates of true strain, $\dot{\varepsilon}_S$, rather than the engineering quantity. Similarly, one might prefer to deal with the true specimen stress, σ_S, instead of the engineering stress. Provided the specimen's volume is conserved during deformation, these modifications are easy to make. Combining the well-known relations

$$\sigma_S = s_S(1 - e_S) , \tag{47}$$

$$\varepsilon_S = -\ln(1 - e_S) , \text{ and} \tag{48}$$

$$\dot{\varepsilon}_S = \frac{\dot{e}_S}{1 - e_S} \tag{49}$$

with equation 46 leads to

$$\sigma_I = \frac{A_S}{A_B} \frac{\sigma_S}{\left[1 + \exp(-\varepsilon_S)\right]} + \frac{L_S \rho c_0}{2} \dot{\varepsilon}_S \left[1 - \exp\left(-\varepsilon_S\right)\right] , \tag{50}$$

where ε_S is obtained from the given $\dot{\varepsilon}_S$ by time integration. This gives the incident pulse necessary to generate a test at the specified rate of true strain (e.g., constant).

The problem with this method is that the behavior of the specimen at the desired rate must be known prior to the test. Since with an uncharacterized material this is not the case, one must first determine this behavior approximately from a test at a similar rate (although not necessarily constant). This information can then be used to design a projectile for a second test. Depending on the rate sensitivity of the material, the rate may still not be sufficiently constant, but it should be closer than the first. It can therefore be used to design an improved projectile for a third test. In this way, the incident pulse can be "fine tuned" in a succession of tests until the desired result is obtained.

4.1 Example–High-Rate Testing of Nylon

As an example, a number of nylon specimens were tested with an aluminum SHPB. The objective is to achieve a test at a constant rate of true strain of 2500 s^{-1} to a total true strain of 0.65. The bars are each 19.05-mm in diameter and 2438-mm long. The specimens were initially cylindrical and nominally 4.76-mm in length and 6.35-mm in diameter. It is assumed that the material conserves volume throughout its deformation.

An initial test series of tests are performed with a uniform cylindrical aluminum projectile (19.05-mm diameter, 610-mm length, impact speed of 11.8 m/s) to obtain a test at an approximate rate of 2500 s^{-1}. A small copper pulse shaper, 0.25-mm thick and 3.18-mm in diameter, is placed between the projectile and incident bar to reduce dispersion. Three tests are conducted for repeatability; the strain signals from one of the tests are shown in figure 3. Note the roughly square pulse that results from the cylindrical striker bar. Figure 4 shows the strain-rate histories for these tests (black lines). Although initially the strain-rate is about 2500 s^{-1}, it increases to almost 3700 s^{-1} by the completion of the test (primarily due to the expansion of the specimen). The resulting stress-strain curves are shown in figure 5 (black lines).

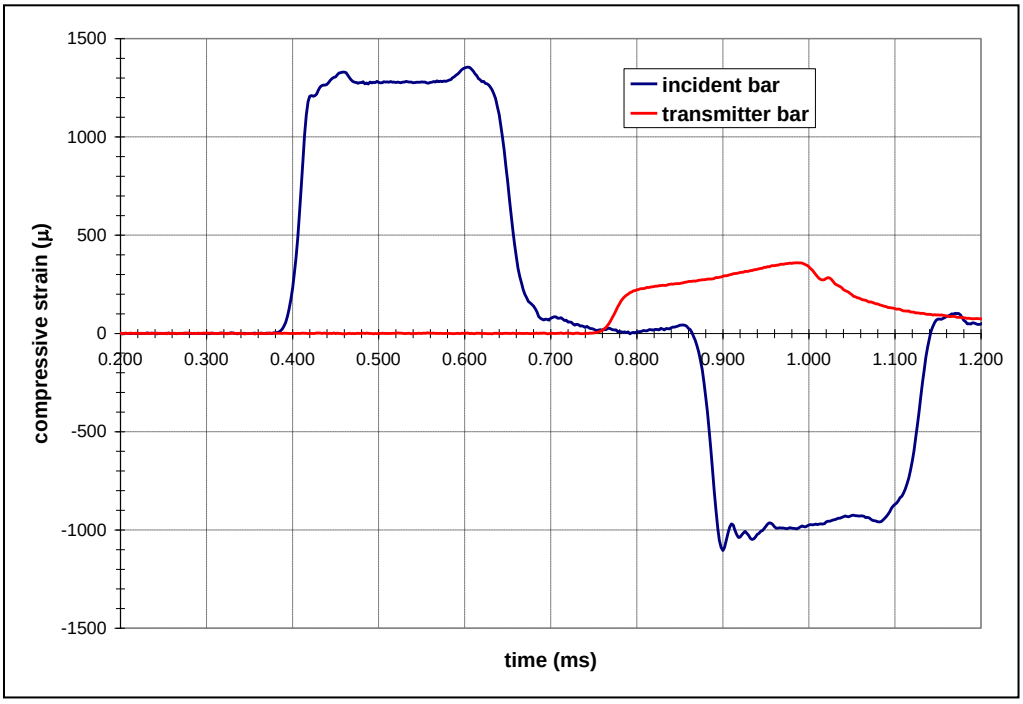

Figure 3. Strain signals from a test on nylon with a uniform projectile. Note the incident pulse is roughly square.

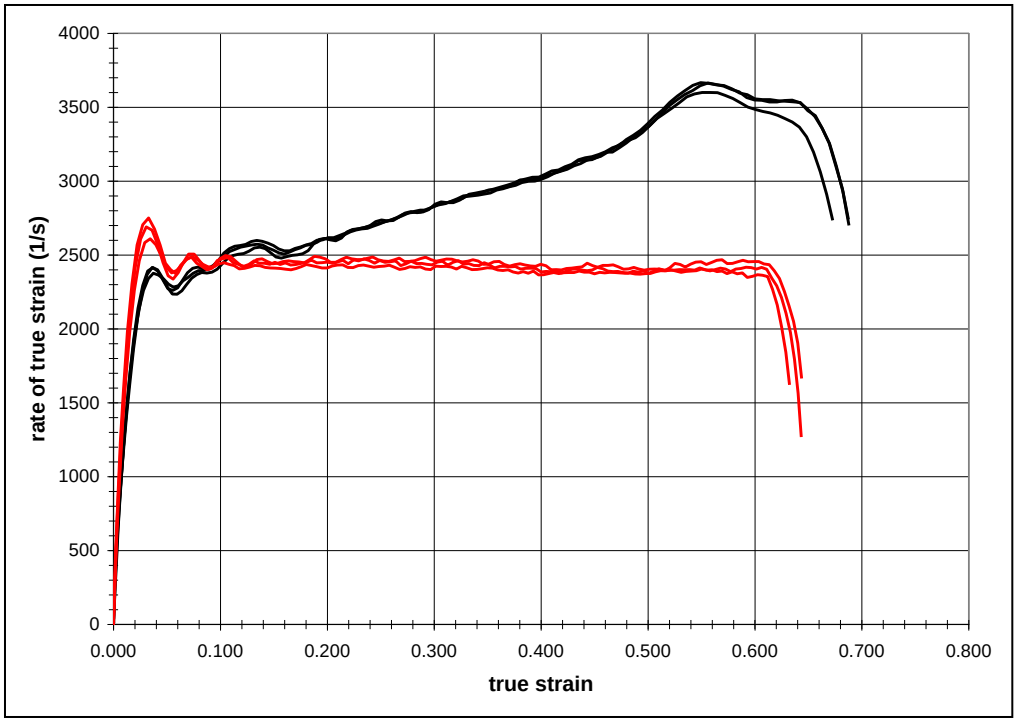

Figure 4. Strain-rate histories from two series of tests on nylon specimens. The first series of tests uses a constant diameter projectile and leads to a non-constant rate. The second series of tests uses a tapered projectile and yields a constant rate.

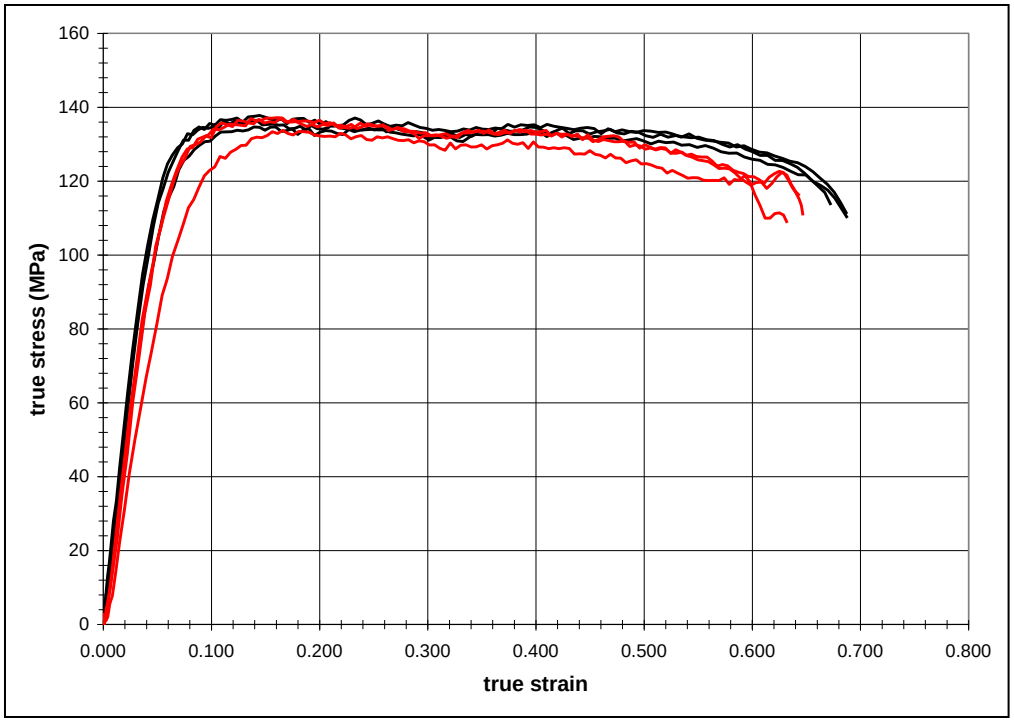

Figure 5. Stress-strain curves for the two series of tests on nylon samples using constant diameter and tapered projectiles.

Next, the specimen response of figure 5 is used in equation 50 to determine the shape of the incident pulse needed to yield a test at a constant rate of 2500 s^{-1}. This signal is shown in figure 6. The method of section 2.2 is then used with an n=20 solution to find the shape of an aluminum striker needed to produce this pulse. This shape is given in figure 7, and it is noted that the maximum diameter matches the diameter of the incident bar. It is interesting to see that the shape of this projectile roughly matches the profile of the incident pulse; however, this is just an observation and there does not seem to be any general implications of this. The projectile made to these dimensions was machined piecewise as depicted. One could machine the shape to a smooth curve that approximates this function but in the present case the projectile contains the steps shown in the figure.

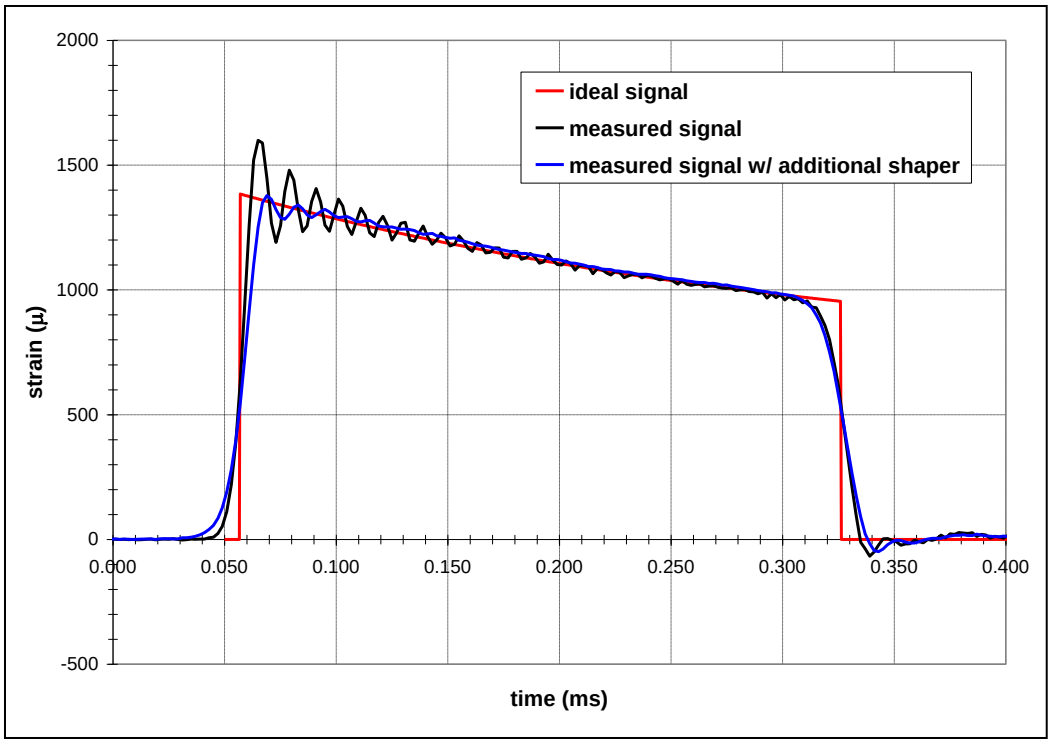

Figure 6. The incident pulse generated by the tapered signal. Except for oscillations due to dispersion, the measured signal (black) matches the desired signal (red) very well. These oscillations can be lessened (blue) through the use of a wave shaper, in this case a small amount of grease. Note this is accompanied by an increase in rise-time.

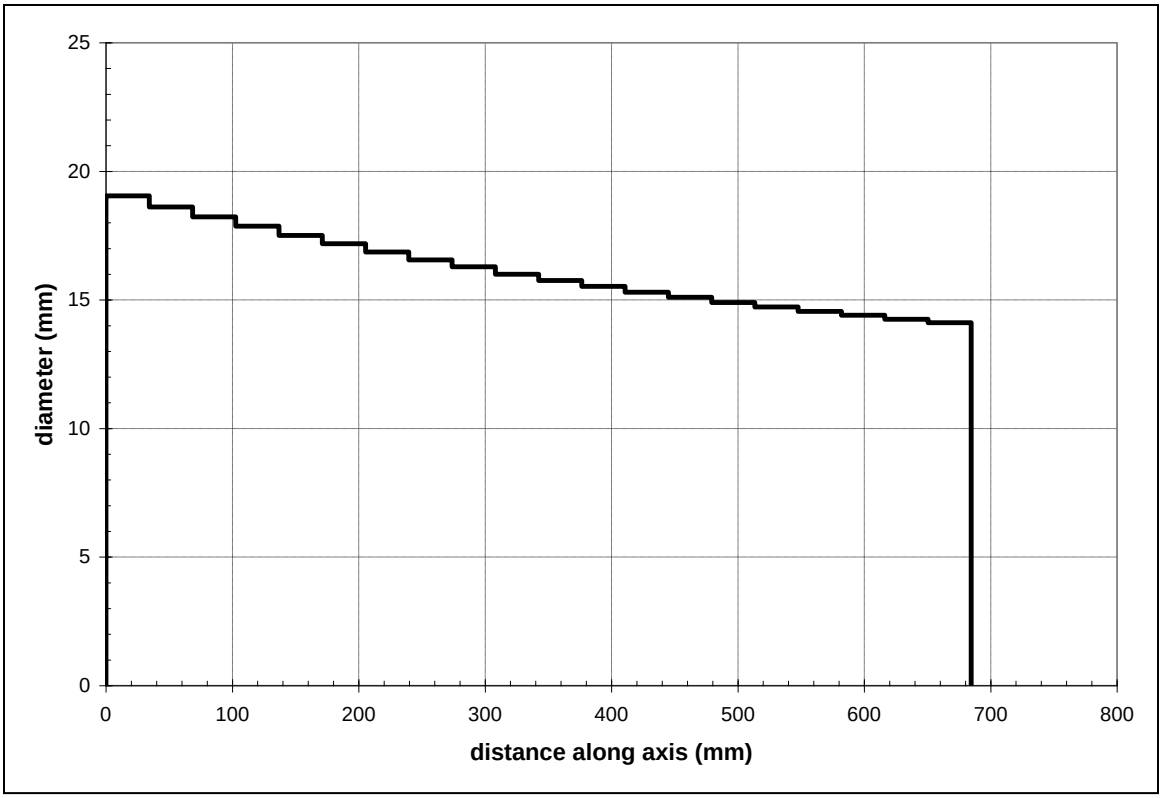

Figure 7. The geometry of the tapered striker needed to yield a constant strain-rate test with the nylon samples as predicted by the synthesis method (n=20) and equation 50.

The actual signal measured by the incident bar strain gage due to impact with this projectile is shown in figure 6. It is noted that, aside from the oscillations stemming from dispersion, the measured signal closely matches the desired signal.[11] Note that it is possible to mitigate these oscillations by using a small pulse shaper as done in the previous series of tests. This is also shown in figure 6, where a second impact is recorded from a test where a small amount of grease was placed between the striker and the incident bar to serve as a wave shaper.

This tapered projectile is next used to test three additional nylon specimens (impact speed of 11.8 m/s). The strain signals for one of these tests are shown in figure 8. As seen previously in figure 6, the incident pulse is ramped to the shape needed to satisfy equation 50. The resulting strain-rates for the tests are shown in figure 4 (red lines). As desired, all three tests are at a uniform rate of 2500 s^{-1}. The resulting stress-strain curves are shown in figure 5 (red curves). We note that there appears to be a measurable difference between the two sets of curves (i.e., those produced from the constant cross-section projectile and those produced from the tapered projectile). However, a larger number of tests would be necessary to confirm whether this is a result of the differing loading histories of the specimens or not.

[11]Also note the pulse terminates after one complete transit of the projectile; there is no "additional" signal that could interfere with the reflection.

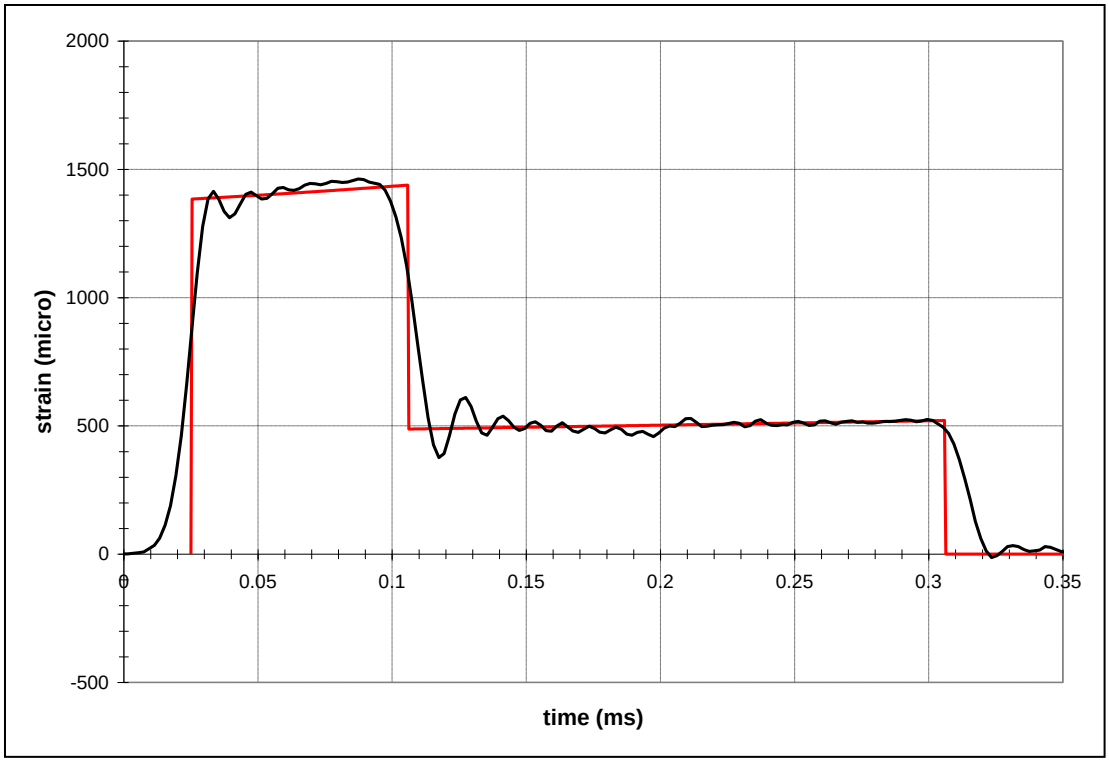

Figure 8. Red–the ideal incident pulse needed to generate a strain-rate jump from 2500 s^{-1} to 500 s^{-1} with a nylon sample. Black–the actual pulse as measured by the strain gages on the incident bar.

4.2 Strain-Rate Jumps

It is possible to apply a modest strain-rate jump to a specimen in a SHPB using a two-part projectile. For example, Leroy et al. (*2*) used two-part projectiles to impart strain rate jumps in copper and aluminum. Gilat and Pao (*17*), developed an analogous procedure with a stepped bar in a torsional SHPB to achieve the same effect. In a similar spirit, Chen and Luo (*18*) used a two part projectile (a higher impedance followed by a lower impedance) to test ceramics in both its uncrushed and crushed form using a single SHPB test. The synthesis method of section 2.2 can easily predict the geometries of such projectiles exactly as shown in the prior example. To show this, consider the nylon material previously discussed. It is desired to conduct a test that would subject a sample to an engineering stain rate of 2500 s^{-1} for a total engineering strain of 0.20, and then instantaneously drop this rate to 500 s^{-1} for an additional 0.10 strain. This incident pulse is plotted in figure 8. The projectile shape needed to produce this pulse, as predicted by the synthesis method with n=30, is shown in figure 9. Again the maximum diameter of the projectile matches the diameter of the SHPB. Although the projectile is divided into two major portions each section contains a slight taper. These tapers are important in that they ensure that each separate loading regime will be applied at a uniform rate. The actual incident pulse, as recorded by the incident bar strain gages, is plotted with the ideal case in figure 8.

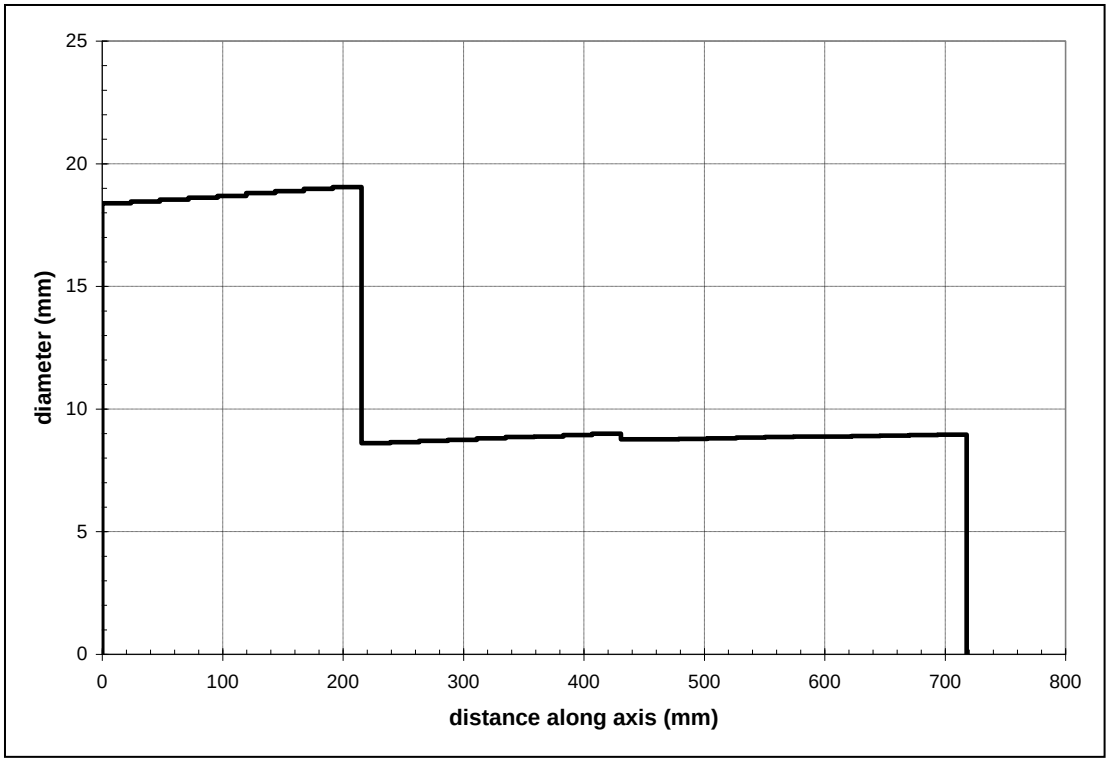

Figure 9. The geometry of the projectile needed to produce the incident pulse shown in figure 8 (to create a strain-rate jump).

The results from a test with this projectile are shown in figure 10. The strain-rate profile is nominally as desired (2500 s^{-1} until 0.20 strain, and 500 s^{-1} until 0.30 strain). In addition, the stress clearly contains a marked decrease corresponding to the drop in rate, and is indicative of the rate-sensitivity of this material.

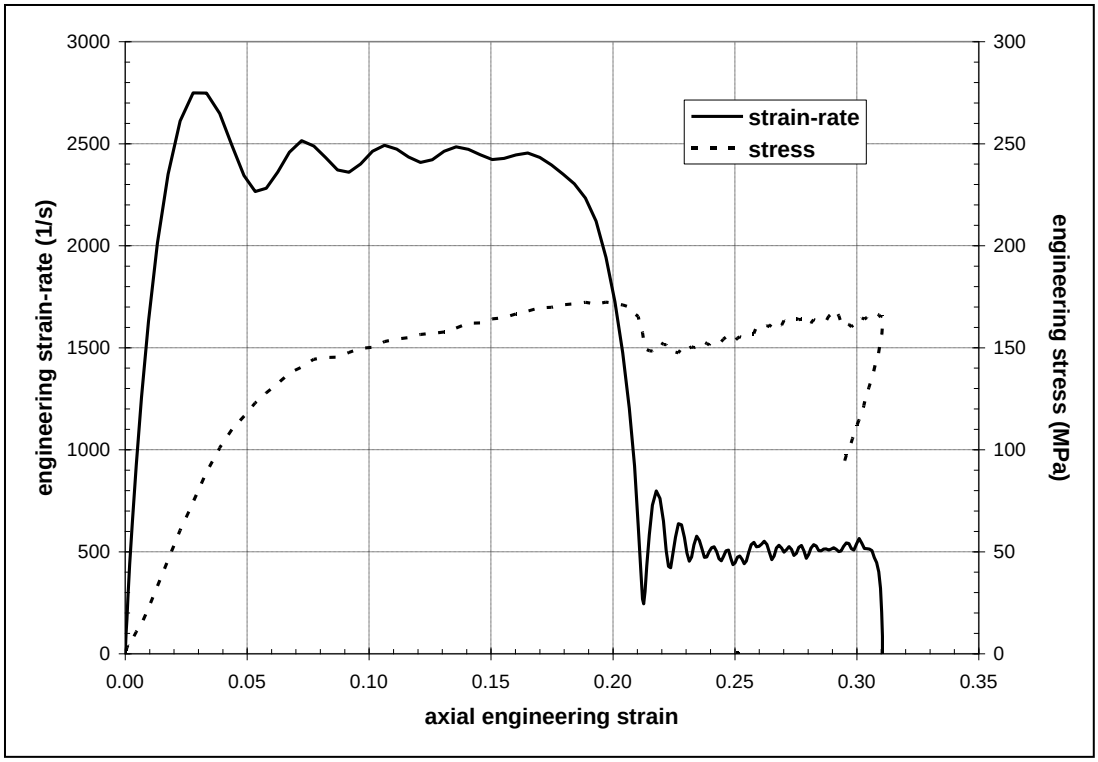

Figure 10. Stress and strain-rate as functions of strain for a strain-rate jump test.

Notice the rate is roughly constant over both rate regimes. Also note the abrupt drop in specimen strength due to the sudden decrease of rate.

5. Discussion and Conclusions

This report has presented an approximate solution to the inverse problem of one-dimensional elastic impact; that is, a solution has been developed that predicts the variation of projectile impedance necessary to produce a desired force-time history on a uniform impedance elastic half-space. The method is approximate in the sense that the desired force history is in general a smooth function but must be approximated by a series of piecewise constant intervals. However, as the method is quick to implement and execute on a digital computer, it is not difficult to use a large enough number of intervals to sufficiently approximate the smooth function for reasonable problems. The primary advantage of this method is that it avoids the trial-and-error approach associated with projectile design based on the forward version of this problem. Thus given a specific impact force history, one can immediately determine the impedance (or shape) of the necessary projectile. An additional advantage is that the method clearly illustrates non-existent

solutions. In other words, it is not possible to create a projectile for every possible force history; one cannot create tension from the impact, for example.[12] This is clearly identified in the output from the routine in the form of negative impedance values for one or more segments. Thus one is spared the fruitless attempt at creating an impossible projectile that sometimes occurs when designing by an analysis based method, like repeated finite element analyses.

To demonstrate its most likely application, the procedure has been used as a pulse-shaping technique for the SHPB. This is a field of growing interest and is usually approached through the use deformable wave-shapers placed at the impact end of the incident bar. In the previous section, pulse-shaping for constant strain rate and for instantaneous strain-rate jumps have been demonstrated using the tapered projectile method. These two specific examples have been chosen because they require signals that are difficult to create using deformable pulse shapers. For example, whereas it is fairly simple to generate a "ramp up" type signal with a pulse shaper, it is more difficult to create the "ramp down" profile shown in figure 6. In addition, the "step" shown in figure 8 would be very difficult to create with deformable pulse shapers, perhaps requiring some type of shaper that exhibits some rapid type of densification, like polymeric or metallic foam. This type of pulse shaper design is difficult to control. Thus the tapered projectile approach is somewhat indispensable for some categories of tests and not simply an alternate approach to more common techniques. Furthermore, tapered projectiles can be used in conjunction with other minor pulse shaping techniques to reduce dispersion. This is seen in figures 6 and 8 where a small copper pad and a small dab of grease were used at the impact end of the incident bar to increase the rise-time of the incident pulse. Likewise, one could achieve a similar effect by slightly rounding the impact end of either the bar or projectile.

As a final note we emphasize that only one-dimensional non-dispersive linear elastic wave propagation has been considered. In many cases with bar impact, dispersion is a problem. With some effort the method could be made to include these effects, and also those due to linear viscoelastic material behavior, by incorporating the framework described by Bacon (*13*). However, it is believed that this would be of little benefit to the types of applications discussed herein.

[12] A better example is the strain-rate jump test previously shown. It can be shown that although it is possible to create a rate jump. of 2500 $^{s-1}$ to 500 $^{s-1}$ with the selected specimen/bar configuration, it is not possible to create a jump of 500 $^{s-1}$ to 2500 $^{s-1}$. To do so would require a projectile with a negative impedance, which is a physical impossibility.

6. References

1. Chen, W.; Lu, F.; Frew, D. J.; Forrestal, M. J. Dynamic Compression Testing of Soft Materials, Transaction of the ASME. *J. of Applied Mechanics* **2002**, *69* (3), 214–223.

2. Leroy, M.; Radd, M.; Nkule, L.; Cheron, R. (1984) *Influence of Instantaneous Dynamic Decremental/Incremental Strain Rate Tests On The Mechanical Behavior Of Metals – Applications To High-Purity Polycrystalline Aluminum*, Inst. Phys. Conf. Ser., No. 70, 31–38.

3. Frew, D. J.; Forrestal, M. J.; Chen, W. A Split Hopkinson Bar Technique to Determine Compressive Stress-Strain Data for Rock Materials. *Experimental Mechanics* **2001**, *41* (1), 40–46.

4. Frew, D. J.; Forrestal, M. J.; Chen, W. Pulse-Shaping Techniques for Testing Brittle Materials With a Split Hopkinson Pressure Bar. *Experimental Mechanics* **2002**, *42* (1), 93–106.

5 Christensen, R. J.; Swanson, S. R.; Brown, W. S. Split-Hopkinson-bar Tests on Rock under Confining Pressure. *Experimental Mechanics* **1972**, *29*, 508–513.

6. Lok, T. S.; Li, X. B.; Liu, D.; Zhao, P. J. Testing and Response of Large Diameter Brittle Materials Subjected to High Strain Rate. *J. of Materials in Civil Engineering* **2002**, *14* (3), 262–269.

7. Lundberg, B.; Lesser, M. On Impactor Synthesis. *J. Sound. Vib* **1978**. *58* (1), 5–14.

8. Mao, M.; Rader, D. Longitudinal Pulse Propagation In Nonunifrom Elastic and Viscoelastic Bars. *Int. J. Solids. Struct.* **1970**, *6*, 519–538.

9. Lundberg, B.; Carlsson, J.; Sundin, K. *Analysis of* Elastic Waves In Non-Uniform Rods From Two-Point Strain Measurement. *J. Sound. Vib* **1990**, *137* (3), 483–493.

10. Bacon, C. Numerical Prediction of the Propagation of Elastic Waves In Longitudinally Impacted Rods: Applications to Hopkinson Testing. *Int. J. Impact Eng.* **1993**, *13* (4), 527–539.

11. Bacon, C. Longitudinal Impact of a Shaped Projectile on a Hopkinson Bar. *J. App. Mech.* **1994**, *61*, 493–495.

12. Nygren, T.; Andersson, L.; Lundberg, B. Optimum Transmission of Extensional Waves Through a Non-Uniform Viscoelastic Junction Between Elastic Bars. *Eur. J. Mech. A/Solids* **1996**, *15*, 29–49.

13. Bacon, C.; Braun, A. Methodology for a Hopkinson Test With a Non-Uniform Viscoelastic Bar. *Int. J. Impact Eng*. **2000**, *24*, 219–230.

14. Liu, D.; Li, X. Dynamic Inverse Design and Experimental Study of Impact Pistons. *Chinese J Mech Engng* **1998**, *34* (4), 506214.

15. Graff, K. *Wave Motion in Elastic Solids*; Dover Publications, Inc.: New York, 1975; 83–84.

16. Meyers, M. *Dynamic Behavior of Materials*; John Wiley and Sons, Inc.: New York, 1994, 305–307.

17. Gilat, A.; Pao, Y. H. High-Rate Decremental Strain-Rate Test. *Experimental Mechanics* **1988**, *28* (3) 322–325.

18. Chen, W.; Luo, H. Dynamic Compressive Responses of Intact and Damaged Ceramics From a Single Split Hopkinson Pressure Bar Experiment. *Experimental Mechanics* **2004**, *44* (3), 295–299.

Appendix. Fortran Routine for Impactor Synthesis

The following FORTRAN program can be used to solve the synthesis problem described in this paper. Variable names are chosen to match those used in the preceding text as closely as possible. Input data is listed directly in the ReadData routine and the output is a list of impedance values for the projectile segments. Note the code is written for clarity and not efficiency. The reader is especially referred to the comments at the end of section 2.2; this code will not run efficiently for large values of n (say n>10 or 20) as it will result in a large amount of repetitive computations. It is therefore advised that at least some rudimentary provision be incorporated to the code that will avoid recalculating the functions F and G during execution.

```
      real z(-100:100),vk(1:100),TR(-100:99),vp
      integer m,n
      integer i,j,k
      real temp0,temp2
      common m,n,vp,vk,z,TR
      call ReadData
      k=0
      do j=1,m,2
        k=k-1
        TR(k)=0
        temp0=F(0,j)
        TR(k)=2
        temp2=F(0,j)
        TR(k)=2*(vk(j)-temp0)/(temp2-temp0)
        z(k)=TR(k)*z(k+1)/(2.0-TR(k))
        print*,k,z(k)
      enddo
      end
*******************************************************************************
      subroutine ReadData
      real z(-100:100),vk(1:100),TR(-100:99),vp
      integer m,n
      integer i,j,k
      common m,n,vp,vk,z,TR
      n=5
      m=2*n
      vp=5.0
      z(0)=1.0
      vk(1)=0.50
      vk(3)=0.55
      vk(5)=0.60
      vk(7)=0.65
      vk(9)=0.70
      return
      end
*******************************************************************************
      real function F(i,j)
      real z(-100:100),vk(1:100),TR(-100:99),vp
      integer m,n
      integer i,j
      common m,n,vp,vk,z,TR
      if((i.ge.1).or.(i.lt.-n))then
          F=0.0
```

```
        else
          if(j.le.-i)then
              F=vp/2.0
            else
              F=F(i-1,j-1)*TR(i-1)+G(i,j-1)*RL(i-1)
          endif
      endif
      return
      end
*******************************************************************************
      real function G(i,j)
      real z(-100:100),vk(1:100),TR(-100:99),vp
      integer m,n
      integer i,j
      common m,n,vp,vk,z,TR
      if((i.ge.0).or.(i.lt.-n))then
          G=0.0
        else
          if(j.le.-i-1)then
              G=vp/2.0
            else
              G=G(i+1,j-1)*TL(i)+F(i,j-1)*RR(i)
          endif
      endif
      return
      end
*******************************************************************************
      real function RL(i)
      real z(-100:100),vk(1:100),TR(-100:99),vp
      integer m,n
      integer i,j
      common m,n,vp,vk,z,TR
        RL=1-TR(i)
      return
      end
*******************************************************************************
      real function RR(i)
      real z(-100:100),vk(1:100),TR(-100:99),vp
      integer m,n
      integer i,j
      common m,n,vp,vk,z,TR
        RR=TR(i)-1
      return
      end
*******************************************************************************
      real function TL(i)
      real z(-100:100),vk(1:100),TR(-100:99),vp
      integer m,n
      integer i,j
      common m,n,vp,vk,z,TR
        TL=2-TR(i)
      return
      end
*******************************************************************************
```

NO. OF COPIES ORGANIZATION

1 (PDF only) DEFENSE TECHNICAL INFORMATION CTR
DTIC OCA
8725 JOHN J KINGMAN RD
STE 0944
FORT BELVOIR VA 22060-6218

1 DIRECTOR
US ARMY RESEARCH LAB
IMNE ALC HRR
2800 POWDER MILL RD
ADELPHI MD 20783-1197

1 DIRECTOR
US ARMY RESEARCH LAB
RDRL CIM L
2800 POWDER MILL RD
ADELPHI MD 20783-1197

1 DIRECTOR
US ARMY RESEARCH LAB
RDRL CIM P
2800 POWDER MILL RD
ADELPHI MD 20783-1197

1 DIRECTOR
US ARMY RESEARCH LAB
RDRL D
2800 POWDER MILL RD
ADELPHI MD 20783-1197

2 CVAD ATO MECHANICAL ENGINEER
RDECOM TARDEC GSS
AMSTA TR S
D TEMPLETON
R RICKERT
6501 E 11 MILE ROAD
ATTN RDTA RS / MS 263
WARREN MI 48397-5000

1 ARMS 3323 PURDUE
W CHEN
701 W STADIUM AVE
WEST LAFAYETTE IN 47907

ABERDEEN PROVING GROUND

24 DIR USARL
RDRL CIM G (BLDG 4600)
RDRL WMM B
P MOY
C RANDOW
G GAZONAS
B CHEESEMAN

NO. OF COPIES ORGANIZATION

C YEN
RDRL WMP B
D CASEM
C HOPPEL
T WEERASOORIYA
C GUNNARSSON
M SCHEIDLER
S BILYK
R BECKER
B LOVE
RDRL WMM D
E CHIN
RDRL WMP D
R DONEY
D KLEPONIS
M ZELLNER
J RUNYEON
RDRL WMP
P BAKER
S SCHOENFELD
RDRL WMP E
D PETTY
D HACKBARTH
M LOVE

INTENTIONALLY LEFT BLANK.